Waste Management 78 (2018) 639–648

Contents lists available at ScienceDirect

Waste Management

journal homepage: www.elsevier.com/locate/wasman

Influence of hydrothermal treatment on the mechanical and environmental performances of mortars including MSWI bottom ash

V. Caprai *, K. Schollbach, H.J.H. Brouwers

Department of Built Environment, Eindhoven University of Technology, Eindhoven 5600 MB, The Netherlands

ARTICLE INFO

Article history:
Received 17 April 2018
Revised 6 June 2018
Accepted 14 June 2018

Keywords:
MSWI bottom ash
Hydrothermal treatment
Sand replacement
Tobermorite
Environmental impact
Mechanical performances

ABSTRACT

Nowadays, in many countries the household waste is more and more incinerated, converting refuse in municipal solid waste incineration bottom ash (MSWI BA). A main concern related to the reuse of BA is linked to the leaching of contaminants, such as heavy metals and salts, to the surrounding environment. To limit this leaching, BA is applied as aggregate in the construction field, since the hydration products of cement are able to immobilize contaminants. Although not always suitable from an environmental point of view, a hydrothermal treatment (HT) can be applied to further increase the contaminants retention, as it stimulates the formation of tobermorite and it densifies the cement matrix. However, not many studies have investigated the influence of HT on cement based mortars and even less have been conducted concerning the optimization of the HT conditions. This study investigates the minimum HT duration for the maximization of mechanical performances and minimization of the environmental impact, for mortars including 25% BA, as sand replacement. The optimal autoclaving duration is found to be 6 h HT, which increases the compressive strength by 30% and it improves the retention of ions as Ba^{2+}, Zn^{2+}, and Cl^{-} by 90%, 60% and 32%, respectively, compared to the standard cured sample. For longer treatment (8 h), the HT is not beneficial, since the leaching of contaminants increases due to the decomposition of reaction products as AFt and AFm.

1. Introduction

Due to the high quantities of refuse produced by the modern lifestyle, the management of municipal solid waste is becoming more and more crucial. Due to the limited availability of space, many European countries apply incineration via Waste-to-Energy plants (WtE) before landfilling, in order to reduce the waste volume (Chimenos et al., 1999; Hjelmar, 1996). After incineration, the obtained by-products consist mostly of bottom ash (BA) (80 wt.%). By 2020, through the Green Deal, the Netherlands aim to limit the number of landfills by recycling 100 wt.% of the MSWI by-products as freely applicable materials. Based on the restrictions introduced by the Soil Quality Decree (SQD), this classification will prohibit the use of BA for road base construction, which was till recently one of the main applications. Moreover, defining stricter leaching thresholds, the SQD makes the application of BA in the construction field even a greater challenge (Tang et al., 2015).

Depending on the chemical composition and size of the BA produced, the possible applications for recycling can vary. In the case of fractions between 1 and 32 mm, many applications involve the use of BA as fine or coarse aggregates in concrete (Cresswell, 2007; Kim and Lee, 2011; Kumar et al., 2014; Lynn et al., 2016; Pera et al., 1997). However, the application of BA is limited by factors such as the high porosity and the low crushing value, contributing to a low strength development as well as to the high leaching of contaminants (Cresswell, 2007; Juric et al., 2006; Kim and Lee, 2011). Washing treatments are not always able to lower the overall content of chlorides, sulfates and heavy metals below the SQD thresholds. Among the strategies for limiting this harmful leaching, the immobilization of these contaminants by solidification in the cementitious paste is often used (Giergiczny and Król, 2008; Gougar et al., 1996; Missana et al., 2017; Vollpracht and Brameshuber, 2016). Depending on the contaminants, the immobilization is not always successful due to their different mobility at high pH, impeding the formation of stable phases.

A more effective immobilization can be achieved by hydrothermal treatment (HT), since it leads to the formation of different reaction products, increases the binder reaction degree (Alawad et al., 2015) and it can modify the pH of the pore solution, lowering the alkaline conditions typical of cement pastes (Xi et al., 1997). The immobilization of these contaminants takes place by the incorporation into the crystal structure, by their physical absorption on

* Corresponding author.
E-mail address: v.caprai@tue.nl (V. Caprai).

https://doi.org/10.1016/j.wasman.2018.06.030
0956-053X/

the surface of the reaction products (Missana et al., 2017), but also due to the matrix densification coming from the high pressure applied (Jing et al., 2007a). Furthermore, HT allows the use of many siliceous materials, inert in standard curing conditions, as supplementary cementitious material (Alawad et al., 2015). Among the reactions under autoclaving conditions, the conversion of C—S—H to tobermorite is reported to be promising for the immobilization of many heavy metal cations (Jing et al., 2007a; Komarneni, 1985). Moreover, tobermorite also favors a higher strength development compensating the low mechanical performances of BA. In previous studies, the hydrothermal treatment proved to be effective for the immobilization in systems containing supplementary materials, such as MSWI BA (Jing et al., 2010, 2007a, 2007b; Peña et al., 2006) and blast furnace slag (Jing et al., 2008). However, the retention of heavy metals but also chlorides and sulfates in standard mortars including BA has not been deeply examined. Moreover, the determination of a minimum curing time for the optimization of the environmental and mechanical performances of the final product has not been investigated. Knowing the optimal autoclaving time can reduce the embodied energy of the produced secondary building material, allowing the use of an advanced technique with the minimum environmental impact.

This study investigates the influence of HT at 11 bars and 190 °C in time (4, 6, 8 h) on standard mortars, where 25% of the sand volume was replaced by washed or unwashed MSWI BA. The influence of HT on the phase formation and the microstructure is evaluated by X-Ray Diffraction (XRD), Scanning Electron Microscope (SEM) and Energy Dispersive X-ray (EDX) measurements. The impact of HT on flexural and compressive strength is measured and compared with standard cured samples. Finally, the environmental impact of the mortars, as "unshaped" (i.e. granular) material (particles below 4 mm) is assessed, based on the Soil Quality Decree.

2. Materials and methods

2.1. Materials

In this study, the bottom ash is provided by Heros Sluiskil (NL) with a size fraction below 4 mm. Fig. 1 shows the treatments performed on the MSWI bottom ash in the incineration plants and on laboratory scale. Initially, the bottom ash is separated in two main streams: coarse (BAC) and fine aggregates size (BAF). BAF is further processed by dry sieving in the laboratory, creating three main fractions: BA-L between 1 and 4 mm, BA-M between 0.250 and 1 mm, and BA-S below 0.25 mm. The only fraction used in this paper is BA-L (marked in grey in Fig. 1) and it will be referred to as BA throughout the paper. The selection of BA-L fraction for the application as fine aggregates is due by the high water demand of the smaller fractions (BA-S and BA-M). Moreover for obtaining comparable results with standard sand (particle size below 2 mm), the BA-L particle size selected for this study ranges only between 1 and 2 mm (Fig. 3a, white area). CEM I 52.5 R (PC) is applied as a binder and inert standard sand (98% SiO_2, Norm sand, ISO 679, EN 196-1) is used as fine aggregate, together with the BA.

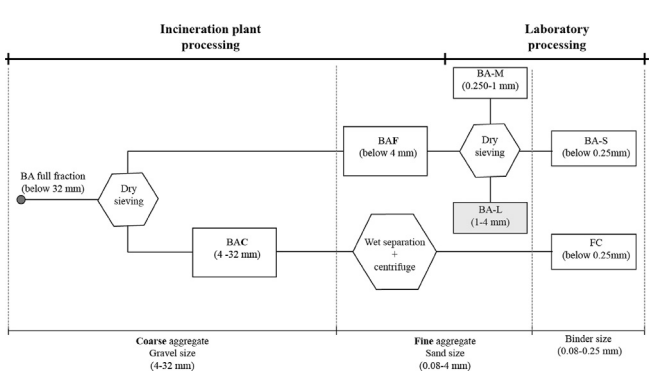

Fig. 1. MSWI bottom ash processing, from the incineration plant to the laboratory.

2.2. Methods

2.2.1. Physical and chemical characterization

In order to avoid modification in the mineral phases, BA is dried at 60 °C for 72 h, for the evaluation of initial moisture content, by mass difference. The overall particle distribution (PSD) is estimated by sieving, using a vibratory sieve shaker (Retsch: AS 450 Basic), according to DIN EN 933-2. The specific density of the BA is measured by Helium pycnometer (AccuPyc II 1340), while a conventional pycnometer is used for determining the bulk density of the loose aggregates. Water absorption measurements are done by determining the mass gain after 24 h of submersion in water. To obtain the saturated surface dry weight, the BA is drained into a 500 μm sieve for 5 min while drying the bottom of the sieve with absorbent paper. Chemical characterization is performed by X-ray Fluorescence (XRF) (PANalytical Epsilon 3 range, standardless OMNIAN method), on pressed powder. The specific surface area and total pore volume are measured using nitrogen adsorption and calculated according to the BET theory (Micromeritics, Tristar II 3020V1.03). The metallic Al content is determined by treatment in alkaline conditions (3 M NaOH solution, for 24 h) (Porciúncula et al., 2012). The flexural and compressive strengths for all the samples are measured according to EN 196-1 (EN 196-1, 2005).

2.2.2. Mortars preparation and treatment curing

The BA is applied as washed and unwashed material (labelled BA and BAw, respectively), in order to evaluate the efficiency of the hydrothermal treatment. The washing procedure is performed by placing distilled water and BA in a container with a liquid to solid ratio (L/S) 3 and using a dynamic shaker for 60 min at 250 rpm, so to maximize the leaching of chlorides and sulfates in these washing conditions (Alam et al., 2017). Mortars are manufactured according to EN 196-1, by using molds with sizes 40 x 40 x 160 mm (EN 196-1, 2005).

Independently of the curing method, 25 vol.% of sand between 1 and 2 mm is replaced by MSWI BA, based on the dry volume of the aggregates. Higher replacement rates are not taken into account due to the decreasing workability of the pastes observed during the mortars casting. The results are then compared with reference samples, made without BA. Before testing for flexural and compressive strength, standard cured mortars are placed in humidified air for 28 days. Curing in water is not carried out, in order to avoid influences on the leaching behavior. Hydrothermally cured mortars are demoulded after 24 h and then treated in an autoclave (Maschinenbau Scholz GmbH & Co. KG, steam generator: WIMA ED36). HT is performed at a pressure of 11 bars and a max temperature of 190 °C, in order to replicate the standard conditions used in the AAC production (190 °C, 11 bars, 8 h). Those conditions ensure the formation of phases as tobermorite, crucial for the increment of strength and reduction of leaching. The entire cycle includes 1.5 h of heating, three different plateau times (1, 3, 5 h) and 1.5 h of cooling, as displayed in Fig. 2 for three total durations of 4, 6 and 8 h. After HT, the samples are further dried in the oven at 40 °C for 15 days, in order to remove the influence of water during the strength evaluation.

The nomenclature of the mortars is as follows: PC_n for the reference, BA_n and BAw_n for the mortars including BA without and with washing treatment, respectively. "n" stands for the curing time (7d, 14d, 28d for standard curing and 4 h, 6 h, 8 h for HT).

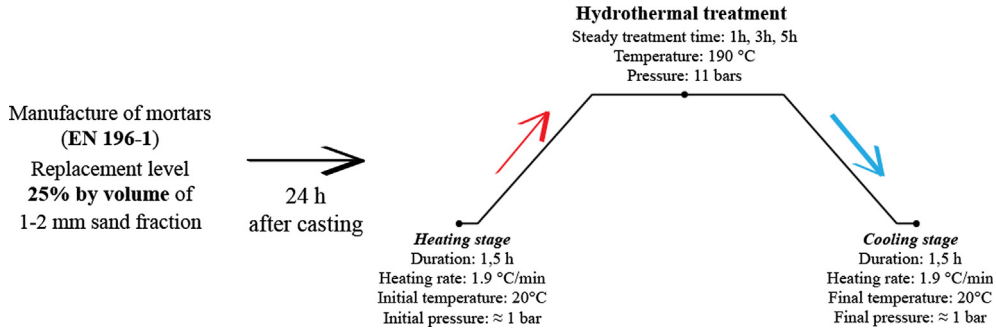

Fig. 2. Graphical representation of the HT methodology applied in the study.

2.2.3. Mineralogical characterization

The identification of crystalline phases before and after the HT is performed by X-ray Powder Diffraction measurements (XRD), with a D2 (Bruker) using a Co tube, fixed divergence slits and a step size of 0.02. The XRD analysis of BA_4h and BA_8h (very similar to BA_6h) are provided as appendix. Before testing, the samples are ground using an agate pestle and mortar, and then sieved below 80 μm. Information about the morphology of the phases and final reaction products are provided by Scanning Electron Microscopy (Phenom ProX). The analysis is performed using a backscattering electron detector with a spot size of 4.0 and a voltage 15.0 kV. Energy-dispersive X-ray spectroscopy (EDX) is carried out using the same settings applied during the Scanning Electron Microscope (SEM) analysis.

2.2.4. Leachability assessment

After mechanical testing, the crushed samples are sieved below 4 mm. The environmental impact of the mortars, as unshaped material is evaluated according to the EN 12457-2 (One stage batch leaching test) (Holm and Hansen, 2003; Florea, 2016), by using a dynamic shaker (ES-SM-30, Edmund Buhler GmbH), in ambient conditions (L/S 10, 250 rpm, 24 h). Previous studies (Caprai et al., 2017; Doudart De La Grée et al., 2016) provided the comparison between the one stage batch leaching test (EN 12457-2) and the column test (Percolation test – NEN 7383:2004), which is generally applied in the SQD (L/S 10, PSD < 4 mm, 21 days). Although the higher accuracy of the column test, the one stage batch leaching test is sufficient for addressing the compliance with legislative limits values (Hage and Mulder, 2004), as leaching obtained from the in batch leaching test overestimates the contaminants concentrations (for the same L/S ratio) (Quina et al., 2011). After filtration by 0.017–0.030 mm membrane filters, chlorides and sulfates are quantified by ion chromatography (IC) (Thermo Scientific Dionex ICS-1100). After acidifying the samples with 0.2% HNO_3, the remaining solutions have been tested for heavy metals by inductively coupled plasma atomic emission spectrometry (ICP-OES), according to NEN 6966 (NEN-EN 6966, 2005). As a reference, the unshaped (granular) materials values from the Dutch soil quality decree (SQD) ("Social Quality Decree," 2015) are used.

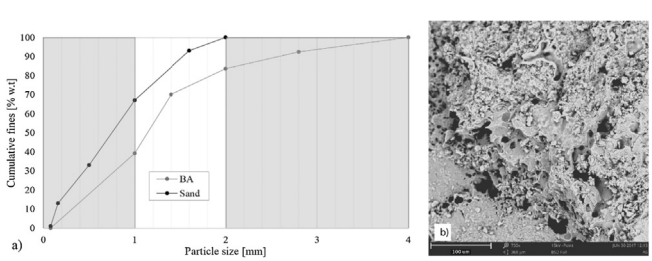

Fig. 3. (a) Particle size distribution of the BA and sand used in the study. Only the fraction 1–2 mm is used as a replacement of sand (white area), (b) morphology of the BA applied in the study.

3. Results and discussions

3.1. Materials characterization

Fig. 3a displays the cumulative PSD of the standard sand and the MSWI BA. Over the selected particle size range (1–2 mm), the BA used is coarser than sand. A comparison of the physical properties of the used aggregates is provided in Table 1. Although it has a similar specific density to sand, BA has a lower bulk density and a much higher surface area. Moreover, the BA exhibits a high total pore volume causing a high water absorption and limiting the applicability in concrete for substitution levels higher than 25 vol.%. These properties are confirmed by the BA morphology (Fig. 3b), characterized by an irregular shape and a visible porous structure.

Due to the treatments applied on this BA fraction in the plant, the amount of metallic Al is minimal, limiting the cracking phenomena related to the hydrogen release in the alkaline environment of PC. No cracking or hydrogen release has been observed during the mortars manufacture.

The chemical composition of the BA before the washing treatment is displayed in Table 2, together with the binder used in the study. The efficiency of the washing treatment to decrease chloride and sulfates leaching on this specific BA is reported elsewhere (Alam et al., 2016). Table 3 displays the environmental impact of the BA before the washing treatment.

Table 1
Physical characterization of the bottom ash in comparison with standard sand.

	Specific Density	Dry bulk density	Water absorption	MC_i^*	Total pore volume	BET Surface area	Metal Al
	g/cm^3	g/cm^3	wt.%	wt.%	cm^3/g	m^2/g	wt.%
BA	2.32	1.14	30.51	16.03	0.0148	4.24	0.13
Sand	2.65	1.49	1.00	0.22	0.0017	0.84	–

* Initial moisture content of the MSWI BA.

Table 2
Oxide composition of the initial (BA) and CEM I 52.5 R (PC), applied in the mortars. RO here indicates the remaining oxides with a concentration lower than 0.1.

	NaO wt.%	MgO wt.%	Al_2O_3 wt.%	SiO_2 wt.%	P_2O_5 wt.%	SO_3 wt.%	K_2O wt.%	CaO wt.%	TiO_2 wt.%	MnO wt.%	Fe_2O_3 wt.%	Cl^- wt.%	RO wt.%	LOI wt.%
BA	1.8	2.1	8.9	22.9	1.8	3.3	1.2	22.5	1.2	0.2	13.1	1.0	1.5	18.5
PC	–	1.5	3.8	15.9	0.5	3.7	0.6	68.9	0.3	0.1	3.6	0.02	0.08	1.00

Heavy Metals

	ZnO	CuO	PbO	Cr_2O_3	BaO	RO
BA	0.6	0.3	0.2	0.1	0.1	0.35
PC	0.12	0.02	–	0.02	–	0.08

Table 3
Leaching limits of inorganic contaminants for unshaped materials. The values given in the SQD are measured by column test (Social Quality Decree, 2015), while the leaching behaviour of the samples was evaluated with the one stage batch leaching test (EN 12475-2). The elements in bold exceed the reference values.

Parameter	SQD Reference Unshaped material mg/kg d.s.	Granular BA mg/kg d.s.
Antimony (Sb)	0.32	**0.61**
Arsenic (As)	0.90	<0.3
Barium (Ba)	22.00	0.63
Cadmium (Cd)	0.04	<0.02
Chromium (Cr)	0.63	0.58
Cobalt (Co)	0.54	<0.02
Copper (Cu)	0.90	**4.41**
Lead (Pb)	2.30	0.42
Molybdenum (Mo)	1.00	0.53
Nickel (Ni)	0.44	0.15
Selenium (Se)	0.15	<0.2
Tin (Sn)	0.40	<0.1
Vanadium (V)	1.80	<0.1
Zinc (Zn)	4.50	2.36
Chloride (Cl)	616.00	**4931.76**
Sulfate (SO_4^{2-})	1730.00	**2333.45**
pH	–	10.2

3.2. Influence of autoclaving on phase composition and microstructure

The phase compositions of all autoclaved mortars containing washed and unwashed BA were determined using X-Ray diffraction and compared to the references without BA (Fig. 4). After 4 h autoclaving, ettringite (AFt) and $Ca(OH)_2$ present in the humid cured samples are no longer detectable in the reference sample (PC_4h), while some unreacted clinker (alite) is still present (Fig. 4a). Compared to PC_28d, all the autoclaved samples show the presence of unidentified peaks at 28.10 and 32.10° 2Theta. They are not considered relevant for the evaluation of the mortar performances, since they are detected independently on the presence of BA in the sample. Qualitatively, PC_6h and PC_8h show the same phase composition as PC_4h. The only observable difference is the slight intensity increase of the tobermorite peak with the increasing of the autoclaving time. This indicates a higher tobermorite content, which fits with the strength development shown in Fig. 7a and b.

From the XRD analysis it is clear that the presence of BA, both washed and unwashed has no visible influence on the phase formation in the autoclaved samples. This is true for all 3 autoclaving times. For this reason only the diffractograms of PC_6h, BA_6h and BAw_6h are shown here (Fig. 4b).

The initial Ca/Si ratio of plain PC (Ca/Si = 4.3) is not favorable for the tobermorite formation in HT conditions (Ca/Si = 0.83) (Galvánková et al., 2016). After the HT on PC mortars, some studies report the formation of α-C_2SH or $C_3SH_{1,5}$, due to the high content of Ca^{2+} in PC mixtures (Alawad et al., 2015). However, in this study, the presence of those phases is not detected, either by XRD or SEM/EDX analysis, whereas tobermorite is. As the samples are not perfectly homogenous mixtures, the higher availability of silica for the tobermorite formation is linked to the partial reaction of the sand fraction creating a lower Ca/Si ratios locally. Fig. 5c displays a quartz grain embedded in the cementitious matrix of sample BA_6h with signs of dissolution on the surface, showing the reactivity of these grains under HT conditions. Further SEM pictures of the autoclaved samples are shown in Fig. 5 for the samples BA_6h and BA_8h. Fig. 5a displays what is likely crystallized C-S-H gel, while Fig. 5b exhibits a pore covered with plate like crystals that could be a zeolite or tobermorite based on the crystal shape. Bulk formation of tobermorite is visible in Fig. 5e. Due to the high porosity and small size of these crystals it was not possible to measure a reliable Ca/Si ratio via EDX.

In BA_8h (Fig. 5d), a phase with a composition close to the zeolite K-Phillipsite $[(K, Na)_2(Si, Al)_8O_{16}{\cdot}4H_2O]$ (Hernandez et al., 1993) was observed in proximity of the BA aggregates. The crystal shape is also similar to the one reported for K-Phillipsite (Gatta et al., 2010). The mineral can form under hydrothermal conditions (Fukui et al., 2009) due to the alkalis supplied by the BA (1.8 wt.% NaO, 1.2 wt.% K_2O). The formation of zeolites during HT, in presence of MSWI BA has been reported in other studies (Deng et al., 2016; Penilla et al., 2003; Temuujin et al., 2002). It is however unusual that no Ca^{2+} could be detected, since K-Phillipsite readily incorporates this element. Since it was not visible with XRD, it is likely that the formation of this phase is a localized phenomenon, not forming in large quantities.

3.3. Mechanical performances of mortars, depending on hydrothermal curing time

Figs. 6 and 7 illustrate the mechanical strength development as a function of time for the standard and hydrothermally cured samples, respectively. In general, the reference samples are able to achieve a higher strength than the ones containing BA. For standard curing, at 28 days, the presence of BA causes a decrease in compressive strength by ≈15% and by ≈9% in flexural strength, compared to the reference (Fig. 6). The presence of BA does not affect qualitatively the reaction products (Section 3.2) and being exposed to the same curing time, the binder reaction degree is comparable among the samples. Therefore, the lower mechanical strength of the mortars including BA can be attributed to the higher porosity of those alternative aggregates compared to the standard sand (Table 1). This is in accordance with other studies (Lynn et al., 2016), where the highly porous structure of BA (Fig. 3b) was resulting in low strength mortars. This phenomenon is mainly related to the localization of the failure in those aggregates, more than in the interfacial transitional zone (ITZ), where it usually occurs (Scrivener et al., 2004). On the other hand, HT improves the mechanical performances with increasing curing time. For the reference sample, the best performance is achieved after 8 h autoclaving, when its flexural and compressive strength improves by 60% and 55%, respectively (Fig. 7c). Compared to the

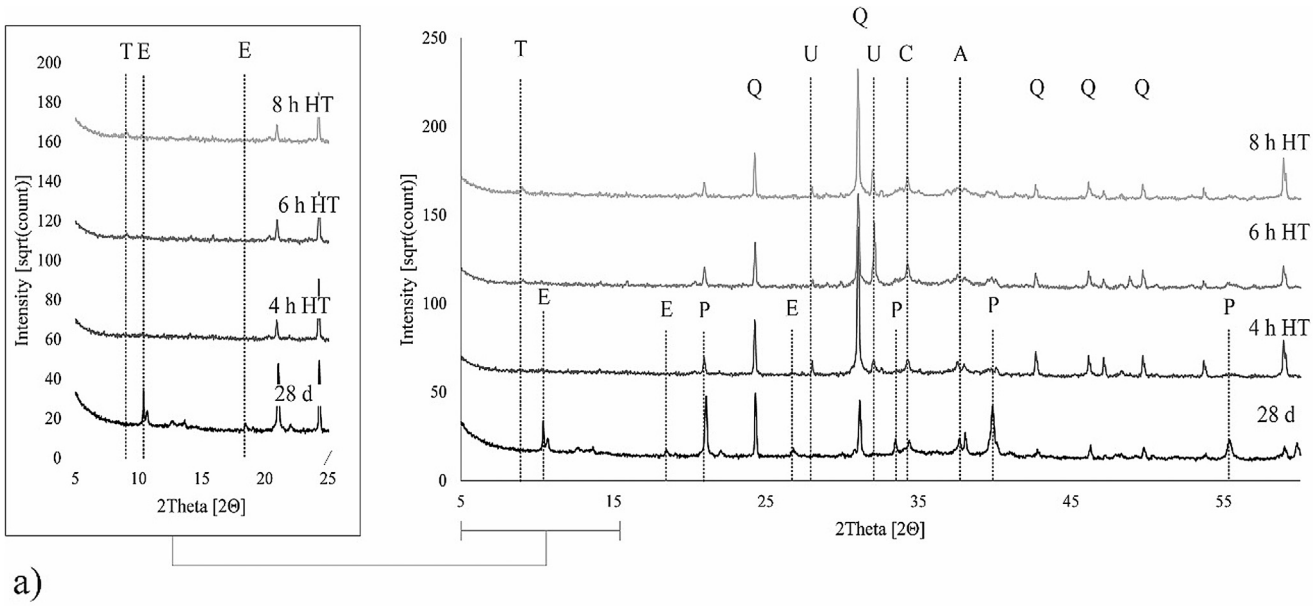

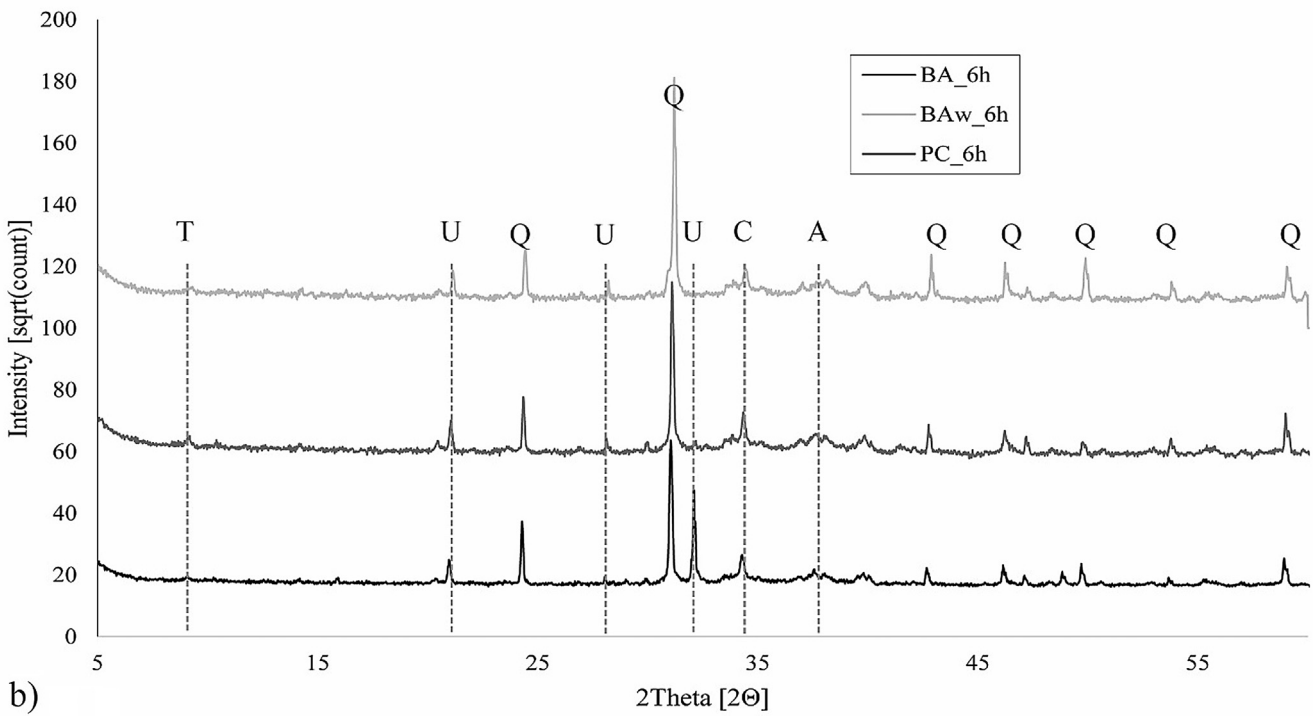

Fig. 4. XRD analysis of references and mortars including 25% of MSWI BA, as a sand replacement: (a) references at different curing time (from the bottom PC_28d, PC_4h, PC_6h, PC_8h and (b) samples after 6 h hydrothermal curing, where PC_6h is the reference standard mortar, BA_6h the mortars with 25 vol.% BA and BAw-6 h the mortars including 25 vol.% BA previously washed. E-ettringite, P-portlandite, Q-quartz, C-calcite, A-Alite, T-tobermorite, U-unknown phase.

BA_28d, the autoclaved mortars including BA are able to achieve higher flexural (19% BA_4h, 45% BA_6h and 54% BA_8h) and compressive strength (5% BA_4h, 25% BA_6h and 29% BA_8h) (Fig. 7c). The main improvement in mechanical properties takes place between 4 and 6 h HT, whereas longer curing times improve the compressive and flexural strength only minimally.

The application of washing treatment on BA appears to affect the final performances of the mortars. In standard conditions (Fig. 6), the washing treatment impacts the early flexural strength positively (BA_7d) and influences the compressive strength only minimally, as the variation is within the experimental error. In autoclaved conditions, the flexural strength is negatively affected (BAw_6h has 21% lower strength than BA_6h), whereas the performances in compressive strength are comparable. The removal of potentially reactive phases from the aggregates surface during washing might lead to a weaker transition zone between the BA aggregates and the cement paste, and therefore to lower strength.

3.4. Leachability assessment of the mortars, depending on the hydrothermal curing time

The leaching of the reference and autoclaved mortars are displayed in Fig. 8, for the contaminants regulated by the SQD which

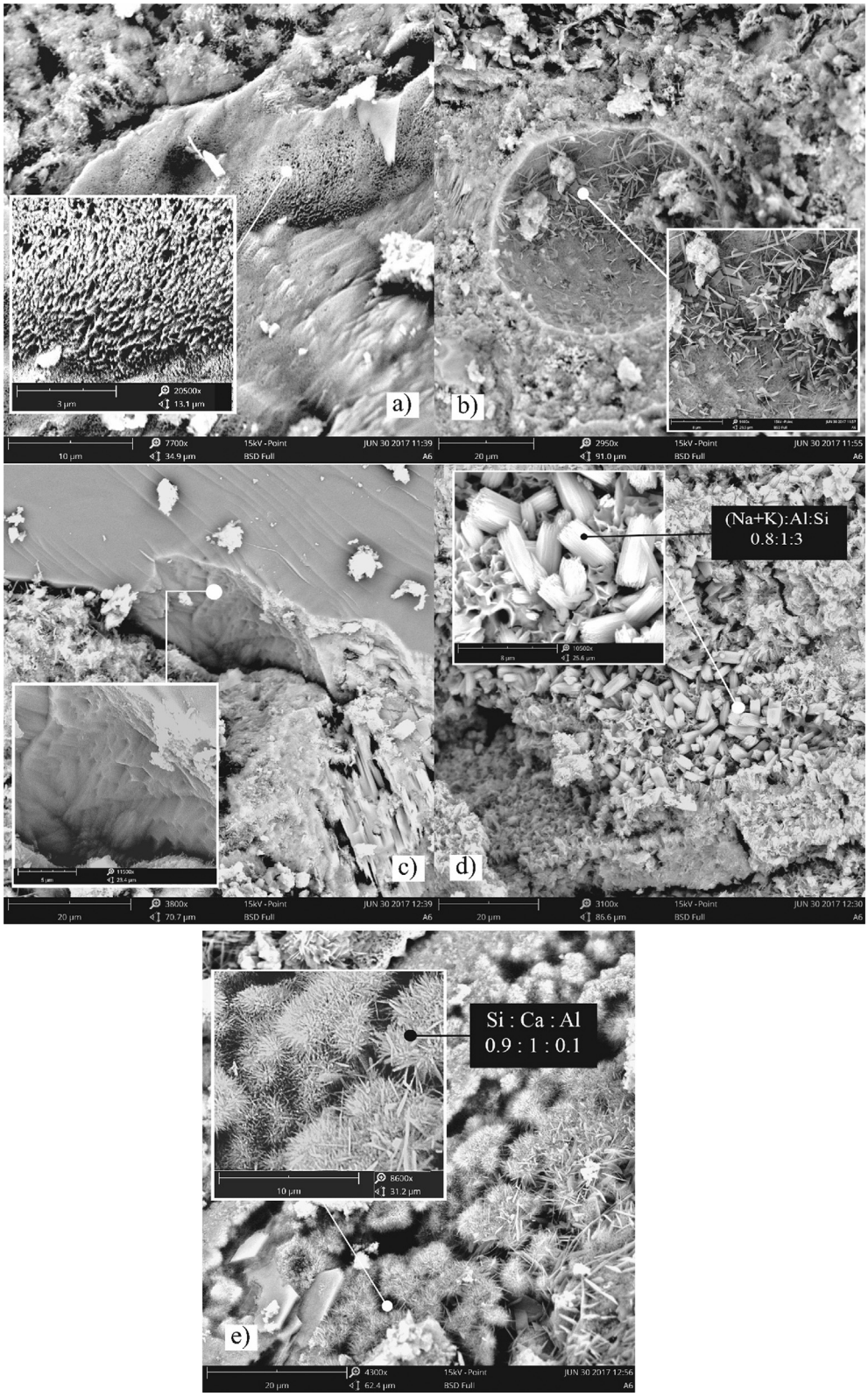

Fig. 5. Morphology of mortars including MSWI BA, for different hydrothermal treatment durations, (a) BA_6h, Crystallized C-S-H gel (b) BA_6h, Tobermorite phase (c) BA_6h, Quartz grain reacting during the HT (d) BA_8h, Na/K Zeolite phase, likely Phillipsite and (e) BA_8h, Tobermorite phase.

showed the highest leachability from the BA as granular material (Table 3, Section 3.1).

Regardless of the curing conditions, the concentrations of all the contaminants are below the threshold values indicated by the SQD. Compared to the BA_28d, 6 h hydrothermal curing reduces the concentrations of Ba, Fe, Cl and Zn, whereas Cu and Cr are unaffected (Fig. 8), and SO_4^{2-} slightly increases (15% higher than BA_28d).

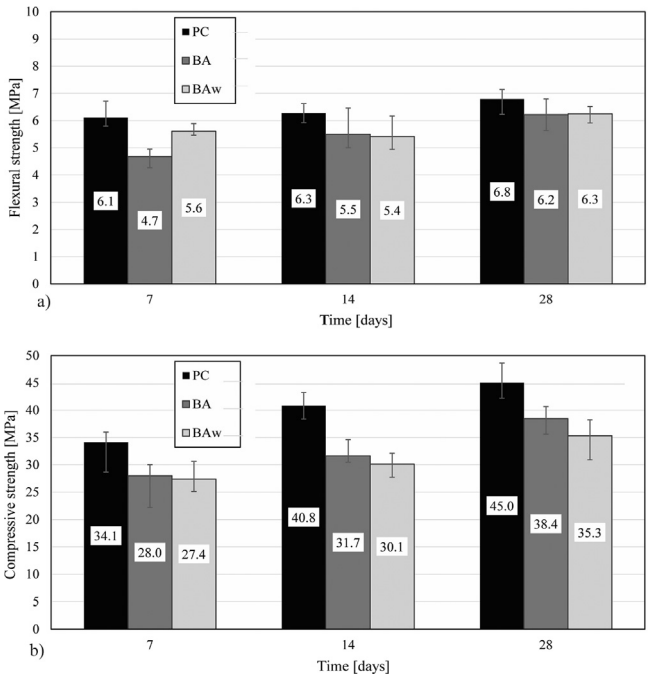

Fig. 6. a) Flexural strength and b) compressive strength of mortars including 25% MSWI BA as a sand replacement. Samples cured in humid conditions and tested as specified by the EN 196-1 (EN 196-1, 2005). *PC* stands for the reference sample, *BA* for the 25 vol.% replacement of unwashed bottom ash and *BAw* for the 25 vol.% washed bottom ash.

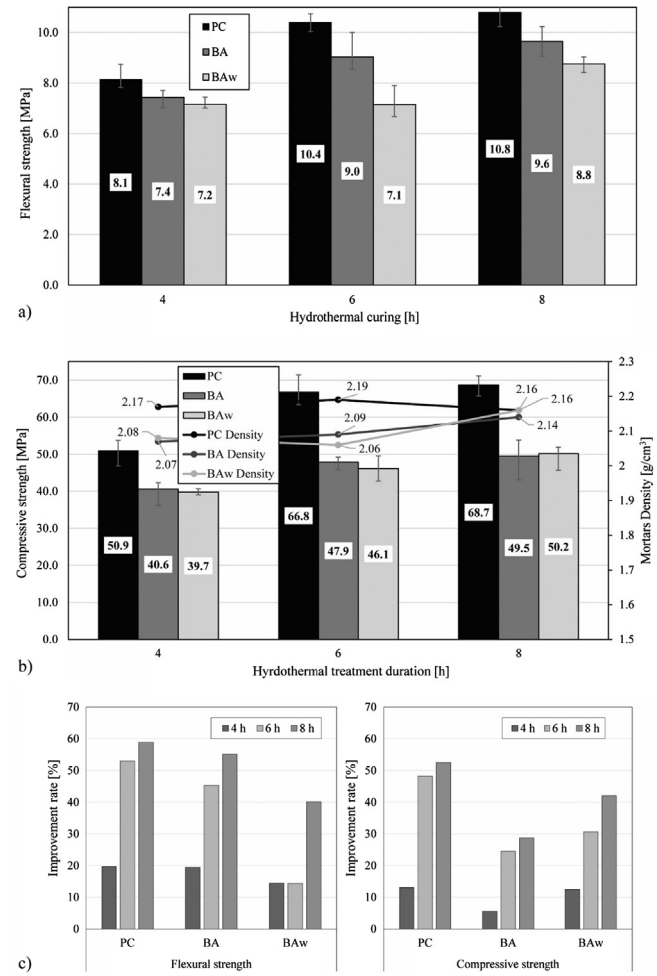

Fig. 7. (a) Flexural strength and (b) compressive strength and density of mortars including 25% MSWI BA as a sand replacement, as function of different HT curing times. (c) Improvement rate based on the reference sample strength at 28 days. Samples tested in oven dry conditions. *PC* stands for the reference sample, *BA* for the 25 vol.% replacement of unwashed bottom ash and *BAw* for the 25 vol.% washed bottom ash.

For a longer curing time (8h), an increase leaching for all the elements is observed.

The HT is very effective for the immobilization of Ba^{2+}. At 4 h HT, BA_4h and BAw_4h leaches 75% less Ba^{2+} than BA_28d and BAw_28d (Fig. 8a), and about 92% less after 6 h HT. The high leaching of Ba^{2+} recorded for BA_28d can depend on different factors. Known the leachability of Ba^{2+} based compounds in high pH (Astrup et al., 2006; Zhang et al., 2016), the application in cementitious systems (pH 12.5) (Florea and Brouwers, 2012), might favor the release of these ions from BA (Keulen et al., 2016). Despite this, the source of Ba^{2+} is often the clinker itself, as this element is incorporated into C_2S or C_3S (Achternbosch et al., 2003; Vollpracht and Brameshuber, 2016). As evaluated by a previous study (Komarneni and Tsuji, 1989), the reduction of the Ba^{2+} leaching after HT is linked to the formation of the tobermorite.

As far as Cu is concerned (Fig. 8b), the leaching from mortars containing washed and unwashed BA is very similar in standard and hydrothermal curing conditions. On the other hand, a reduction of 60% in the leaching of Zn is observed (Fig. 8d) (BA_6h has leaching of 0.09 mg/kg while BA_28d has 0.23 mg/kg). However, after 8 h HT, the leaching of Cu, Fe, total Cr and Zn increases. It appears that particles containing these elements, such as iron oxides, are incorporated into the matrix of the mortar and only start reacting after 8 h HT (Wei et al., 2011).

The sulfate leaching (Fig. 8c) is only minimally influenced by the HT up to 6 h curing. However, the further increase of the HT time to 8 h leads to 4 times higher SO_4^{2-} leaching, indicating possible modifications of the phases incorporating sulfates. Under normal curing conditions, most of the sulfate involved in the reaction of PC precipitate as ettringite within the early stages of hydration (Gougar et al., 1996). In PC_28d, BA_28d and BAw_28d, the amount of ettringite (AFt, $3CaO{\cdot}Al_2O_3{\cdot}3CaSO_4{\cdot}32H_2O$, (Baur et al., 2004)) is minimal, due to its conversion into mono-sulfate (AFm, $3CaO{\cdot}Al_2O_3{\cdot}CaSO_4{\cdot}12H_2O$, (Baur et al., 2004)) during the 28 days standard curing (Locher et al., 1976). The leaching of SO_4^{2-} from the samples PC_28d and BA_28d is 4.1 ± 0.5 mg/l and 3.2 ± 0.5 mg/l, respectively and it is mainly related to the presence of the formed AFm.

On the other hand, ettringite is present in the mortars before the beginning of the HT, since they are cast and demolded after 24 h (Locher et al., 1976). A previous study (Satava and Veprek, 1975) highlights that at temperatures higher than 111 °C, the thermal decomposition of ettringite occurs. The AFt turns firstly in AFm hydrate (C_4ASH_{12}), and from 190 °C up the decomposition of the AFm into hydro-garnet (C_3AH_6, Katoite) and anhydrite II is observed (Satava and Veprek, 1975). In this study, this phenomenon is supported by the XRD measurements where ettringite is no longer visible in the autoclaved samples. It is important to remember that the HT time represents the whole cycle duration, including 1.5 h heating and 1.5 h cooling. Accordingly, the effective plateau at 190 °C lasts 1 h, 3 h and 5 h, for the selected curing time. During the first 6 h of HT, the samples maintain the leaching stable at 3.9 ± 0.5 mg/l matching the solubility of the 28 days cured samples. After 8 h HT the leaching increases, which can be explained by the different solubility between AFm and anhydrite II (Locher et al., 1976; Satava and Veprek, 1975).

A similar trend is observed in chlorides leaching (Fig. 8c), where 6 h HT reduces the leaching by 32%, while the prolonged

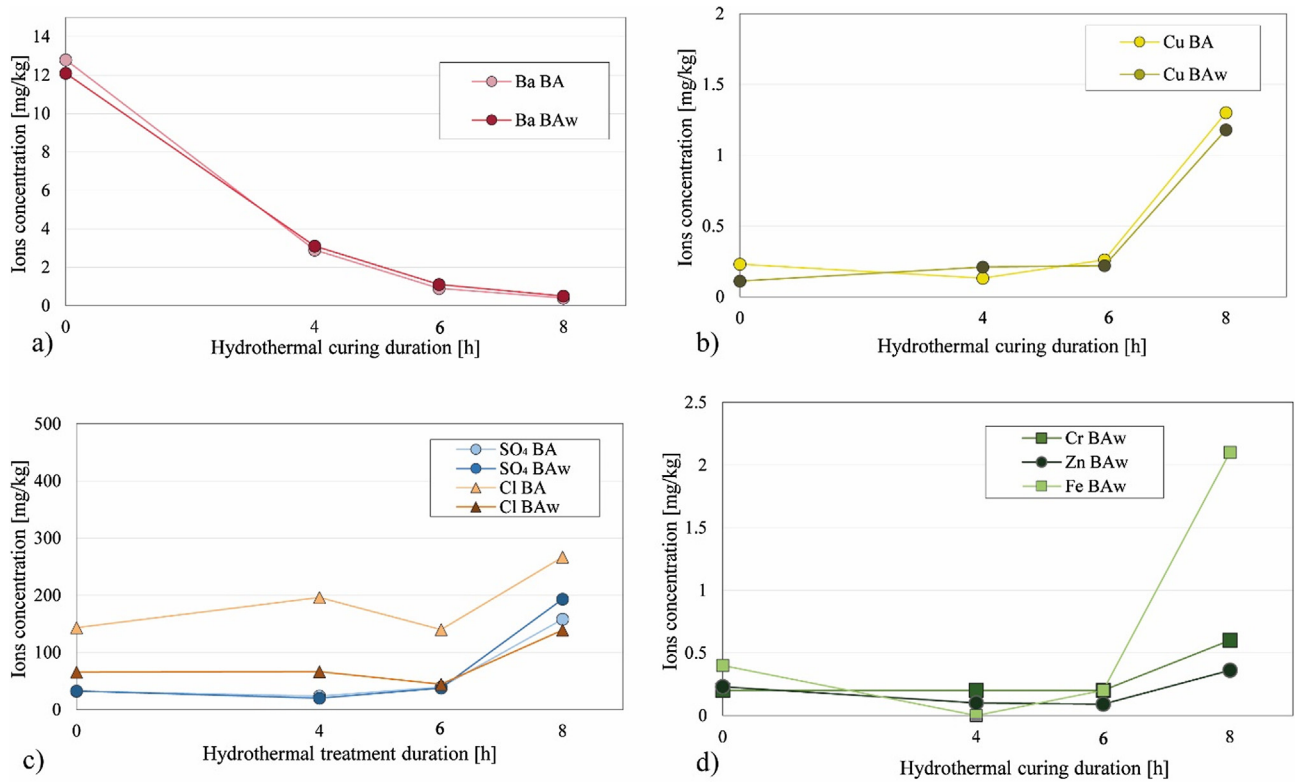

Fig. 8. Concentration of the most leachable elements per kg of MSWI BA, overcoming the SQD legislation limit. (a) Barium, (b) Copper, (c) Zinc and Chromium and Iron, (d) Sulfate and Chloride concentrations. The 0 h HT duration represents the standard cured samples (28 days).

HT (BA_8h) increases it by 86% compared to the standard curing conditions (BA_28d). Among the reaction products in PC hydration, AFt and AFm phases are well known for their chloride binding capacity (Florea and Brouwers, 2012; Larsen, 1998; Zibara, 2001). Therefore, the decomposition of AFm phases previously described could be related to the chlorides leaching trend, as part of those ions are released during the conversion of AFm hydrate to hydrogarnet and anhydrite II.

The washing treatment applied to BA only has an influence in the case of chlorides, where a lower ions concentration is detected from the washed samples. However in both cases the concentration is below the SQD limit as unshaped material. For the other ions, the leaching of mortars containing washed and unwashed BA have very similar trends, meaning a constant retention level independently on the initial concentration. This behavior can indicate that the incorporation of these elements is taking place in the same hydrated phases and resulting in the same dissolution behavior.

4. Conclusions

This study investigates the influence of hydrothermal treatment (HT) on the mechanical and environmental properties of mortars, based on 25 vol.%. BA replacement of standard sand. The following conclusions can be drawn:

- Hydrothermal treatment is beneficial for the developing of higher flexural and compressive strength compared to standard curing. A 6 h HT is optimal to enhance the mechanical and environmental performances of the mortars and to minimize the embodied energy of the final product, at the same time.
- The efficiency of the HT relies on the densification of the matrix and the development of crystalline reaction products (such as tobermorite). A 54% increase in flexural and 29% in compressive strength can be achieved, compared to standard cured samples.
- The presence of BA does not affect the final reaction products visible with XRD. The silica-based compounds such as standard sand and BA particles participate in the reaction, due to the extreme conditions of HT.
- Environmentally, HT is effective for the immobilization of contaminants achieving the optimal conditions after 6 h HT and fulfilling the limitation of the SQD for all the heavy metals, chlorides and sulfates. Ba^{2+} is the most affected by HT, decreasing its leaching by 90%. Although still below the SQD limit, longer HT duration leads to a higher leaching for most of the contaminants.
- Except for chlorides, the washing treatment of BA before the HT had no influence on lowering the leaching of the contaminants.

Acknowledgement

The authors would like to acknowledge the financial support provided by NOW domain Applied and Engineering Science, formally STW (Stichting voor de Technische Wetenschappen), the Netherlands, under the project number 10019729: "Environmental concrete based on treated MSWI bottom ash". Moreover, for equipment support the authors would like to acknowledge the group Chemical Engineering and Chemistry, Chemical Reactor Engineering, Eindhoven University of Technology.

Appendix A

See Fig. A1.

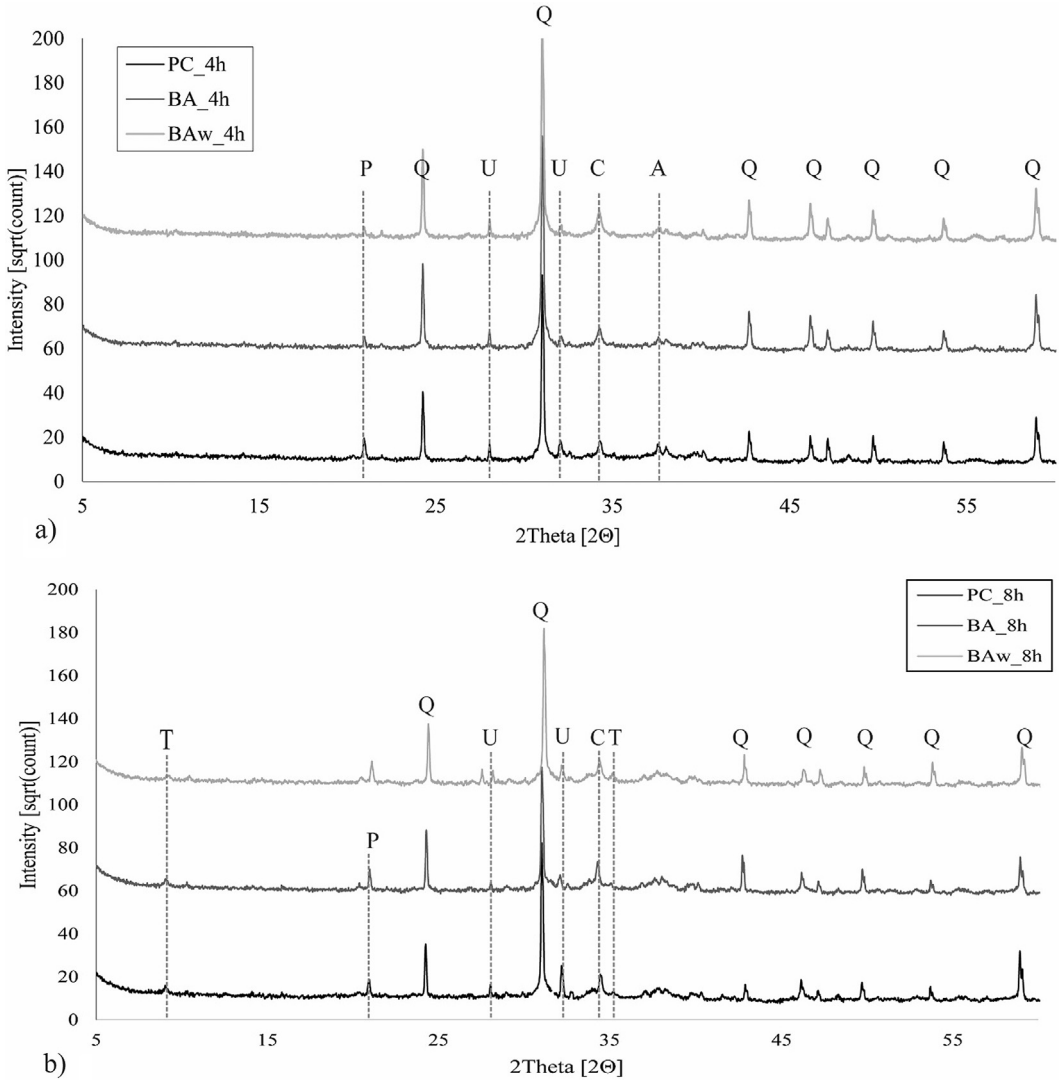

Fig. A1. XRD analysis and comparison among references and mortars including 25% of MSWI BA, as a sand replacement: (a) samples after 4 h (b) 8 h hydrothermal curing. E-ettringite, P-portlandite, Q-quartz, C-calcite, A-Alite, T-tobermorite, U-unknown phase.

References

Achternbosch, M., Bräutigam, K.-R., Hartlieb, N., Kupsch, C., Richers, U., Stemmermann, P., Gleis, M., 2003. Heavy metals in cement and concrete resulting from the co-incineration of wastes in cement kilns with regard to the legitimacy of waste utilisation. Wissenschaftliche Berichte (FZKA-6923) 1–200.

Alam, Q., Schollbach, K., Florea, M.V.A., Brouwers, H.J.H., 2016. Investigating washing treatment to minimize leaching of chlorides and heavy metals from MSWI bottom ash. In: 4th International Conference on Sustainable Solid Waste Management. Limassol, Cyprus.

Alam, Q., Florea, M.V.A., Schollbach, K., Brouwers, H.J.H., 2017. A two-stage treatment for Municipal Solid Waste Incineration (MSWI) bottom ash to remove agglomerated fine particles and leachable contaminants. Waste Manage. 67, 181–192. https://doi.org/10.1016/j.wasman.2017.05.029.

Alawad, O.A., Alhozaimy, A., Jaafar, M.S., Aziz, F.N.A., Al-Negheimish, A., 2015. Effect of autoclave curing on the microstructure of blended cement mixture incorporating ground dune sand and ground granulated blast furnace slag. Int. J. Concr. Struct. Mater. 9, 381–390. https://doi.org/10.1007/s40069-015-0104-9.

Astrup, T., Dijkstra, J.J., Comans, R.N.J., Van Der Sloot, H.A., Christensen, T.H., 2006. Geochemical modeling of leaching from MSWI air-pollution-control residues. Environ. Sci. Technol. 40, 3551–3557. https://doi.org/10.1021/es052250r.

Baur, I., Keller, P., Mavrocordatos, D., Wehrli, B., Johnson, C.A., 2004. Dissolution-precipitation behaviour of ettringite, monosulfate, and calcium silicate hydrate. Cem. Concr. Res. 34 (2), 341–348.

Caprai, V., Florea, M.V.A., Brouwers, H.J.H., 2017. Evaluation of the influence of mechanical activation on physical and chemical properties of municipal solid waste incineration sludge. J. Environ. Manage. 1–12. https://doi.org/10.1016/j.jenvman.2017.05.024.

Chimenos, J.M., Segarra, M., Fernández, M.a., Espiell, F., 1999. Characterization of the bottom ash in municipal solid waste incinerator. J. Hazard. Mater. 64, 211–222. https://doi.org/10.1016/S0304-3894(98)00246-5.

Cresswell, D., 2007. Municipal Waste Incinerator Ash in manufactured Aggregate 1–8.

Deng, L., Xu, Q., Wu, H., 2016. Synthesis of zeolite-like material by hydrothermal and fusion methods using municipal solid waste fly ash. Proc. Environ. Sci. 31, 662–667. https://doi.org/10.1016/j.proenv.2016.02.122.

Doudart De La Grée, G.C.H., Florea, M.V.A., Keulen, A., Brouwers, H.J.H., 2016. Contaminated biomass fly ashes - Characterization and treatment optimization for reuse as building materials. Waste Manage. 49, 96–109. https://doi.org/10.1016/j.wasman.2015.12.023.

EN 196-1, 2005. Method for testing cement - Part 1: Determination of strength.

EN 196-1, B., 2005. Methods of testing cement, Part 1: Determination of strength. http://doi.org/10.1111/j.1748-720X.1990.tb01123.x

Florea, M.V.A., 2016. Environmental interactions of cement-based products. In: Int. Conf. Adv. Cem. Concr. Technol. Africa, Dar es Salaam, Tanzania, accepted in October 2015.

Florea, M.V.A., Brouwers, J., 2012. Chloride binding related to hydration products part I: Ordinary Portland cement. RILEM Bookseries 3, 125–131. https://doi.org/10.1007/978-94-007-2703-8_13.

Fukui, K., Katoh, M., Yamamoto, T., Yoshida, H., 2009. Utilization of NaCl for phillipsite synthesis from fly ash by hydrothermal treatment with microwave heating. Adv. Powder Technol. 20, 35–40. https://doi.org/10.1016/j.apt.2008.10.007.

Galvánková, L., Másilko, J., Solný, T., Štěpánková, E., 2016. Tobermorite synthesis under hydrothermal conditions. Procedia Eng. 151, 100–107. https://doi.org/10.1016/j.proeng.2016.07.394.

Gatta, G.D., Cappelletti, P., Langella, A., 2010. Crystal-chemestry of Philipsites from the Neapolitan Yellow tuff. Eur. J. Mineral. 22, 779–786.
Giergiczny, Z., Król, A., 2008. Immobilization of heavy metals (Pb, Cu, Cr, Zn, Cd, Mn) in the mineral additions containing concrete composites. J. Hazard. Mater. 160, 247–255. https://doi.org/10.1016/j.jhazmat.2008.03.007.
Gougar, M.L.D., Scheetz, B.E., Roy, D.M., 1996. Ettringite and C-S-H Portland cement phases for waste ion immobilization: a review. Waste Manage. 16, 295–303. https://doi.org/10.1016/S0956-053X(96)00072-4.
Hage, J.L.T., Mulder, E., 2004. Preliminary assessment of three new European leaching tests. Waste Manage. 24, 165–172. https://doi.org/10.1016/S0956-053X(03)00129-6.
Hernandez, J.E.G., del Pino, J.S.N., Martin, M.M.G., Reguera, F.H., Losada, J.A.R., 1993. Zeolites in pyroclastic deposits in southeastern tenerife (Canary Islands). Clays Clay Miner. 41, 521–526. https://doi.org/10.1346/CCMN.1993.0410501.
Hjelmar, O., 1996. Disposal strategies for municipal solid waste incineration residues. J. Hazard. Mater. 47, 345–368. https://doi.org/10.1016/0304-3894(95)00111-5.
Holm, J., Hansen, J.B., 2003. CEN EN 12457 leaching test: Comparison of test results obtained by part 1 and 2 with test results obtained by part 3 Dorthe Lærke Baun Jesper Holm Jette Bjerre Hansen Margareta Wahlström.
Jing, Z., Jin, F., Hashida, T., Yamasaki, N., Ishida, E.H., 2008. Influence of tobermorite formation on mechanical properties of hydrothermally solidified blast furnace slag. J. Mater. Sci. 43, 2356–2361. https://doi.org/10.1007/s10853-007-2025-8.
Jing, Z., Jin, F., Yamasaki, N., Ishida, E.H., 2007a. Hydrothermal synthesis of a novel tobermorite-based porous material from municipal incineration bottom ash. Ind. Eng. Chem. Res. 46, 2657–2660. https://doi.org/10.1021/ie070016z.
Jing, Z., Matsuoka, N., Jin, F., Hashida, T., Yamasaki, N., 2007b. Municipal incineration bottom ash treatment using hydrothermal solidification. Waste Manage. 27, 287–293. https://doi.org/10.1016/j.wasman.2006.01.015.
Jing, Z., Ran, X., Jin, F., Ishida, E.H., 2010. Hydrothermal solidification of municipal solid waste incineration bottom ash with slag addition. Waste Manage. 30, 1521–1527. https://doi.org/10.1016/j.wasman.2010.03.024.
Juric, B., Hanzic, L., Ilić, R., Samec, N., 2006. Utilization of municipal solid waste bottom ash and recycled aggregate in concrete. Waste Manage. 26, 1436–1442. https://doi.org/10.1016/j.wasman.2005.10.016.
Keulen, A., Van Zomeren, A., Harpe, P., Aarnink, W., Simons, H.A.E., Brouwers, H.J.H., 2016. High performance of treated and washed MSWI bottom ash granulates as natural aggregate replacement within earth-moist concrete. Waste Manage. 49, 83–95. https://doi.org/10.1016/j.wasman.2016.01.010.
Kim, H.K., Lee, H.K., 2011. Use of power plant bottom ash as fine and coarse aggregates in high-strength concrete. Constr. Build. Mater. 25, 1115–1122. https://doi.org/10.1016/j.conbuildmat.2010.06.065.
Komarneni, S., 1985. Heavy metal removal from aqueous solutions by tobermorites and zeolites. Nucl. Chem. Waste Manage. 5, 247–250. https://doi.org/10.1016/0191-815X(85)90001-4.
Komarneni, S., Tsuji, M., 1989. Selective cation exchange in substituted tobermorites. J. Am. Ceram. Soc. 72, 1668–1674. https://doi.org/10.1111/j.1151-2916.1989.tb06301.x.
Kumar, D., Gupta, A., Ram, S., 2014. Uses of bottom ash in the replacement of fine aggregate for making concrete. Int. J. Curr. Eng. Technol. 4, 3891–3895.
Larsen, C., 1998. Chloride Binding in Concrete-Effect of Surrounding Environment and Concrete Composition. The Norwegian University of Science and Technology.
Locher, F.W., Richartz, W., Sprung, S., 1976. Setting of cement-Part I. Reaction and development of structure. Zement, Kalk, Gyps 29, 435–442.
Lynn, C.J., Dhir OBE, R.K., Ghataora, G.S., 2016. Municipal incinerated bottom ash characteristics and potential for use as aggregate in concrete. Constr. Build. Mater. 127, 504–517. http://doi.org/10.1016/j.conbuildmat.2016.09.132.
Missana, T., García-Gutiérrez, M., Mingarro, M., Alonso, U., 2017. Analysis of barium retention mechanisms on calcium silicate hydrate phases. Cem. Concr. Res. 93, 8–16. https://doi.org/10.1016/j.cemconres.2016.12.004.
NEN-EN 6966, 2005. Milieu - Analyse van geselecteerde elementen in water, eluaten en destruaten - Atomaire emissiespectrometrie met inductief gekoppeld plasma. The Netherlands.
Peña, R., Guerrero, A., Goñi, S., 2006. Hydrothermal treatment of bottom ash from the incineration of municipal solid waste: retention of Cs(I), Cd(II), Pb(II) and Cr(III). J. Hazard. Mater. 129, 151–157. https://doi.org/10.1016/j.jhazmat.2005.08.024.
Penilla, R.P., Bustos, A.G., Elizalde, S.G., 2003. Zeolite synthesized by alkaline hydrothermal treatment of bottom ash from combustion of municipal solid wastes. J. Am. Ceram. Soc. 86, 1527–1533. https://doi.org/10.1002/chin.200350243.
Pera, J., Coutaz, L., Ambroise, J., Chababbet, M., 1997. Use of incinerator bottom ash in concrete. Cem. Concr. Res. 27, 1–5. https://doi.org/10.1016/S0008-8846(96)00193-7.
Porciúncula, C.B., Marcilio, N.R., Tessaro, I.C., Gerchmann, M., 2012. Production of hydrogen in the reaction between aluminum and water in the presence of NaOH and KOH. Brazil. J. Chem. Eng. 29, 337–348. https://doi.org/10.1590/S0104-66322012000200014.
Quina, M.J., Bordado, J.C.M., Quinta-Ferreira, R.M., 2011. Percolation and batch leaching tests to assess release of inorganic pollutants from municipal solid waste incinerator residues. Waste Manage. 31, 236–245. https://doi.org/10.1016/j.wasman.2010.10.015.
Satava, V., Veprek, O., 1975. Thermal decomposition of ettringite under hydrothermal conditions. J. Am. Ceram. Soc. 73, 357–359.
Scrivener, K.L., Crumbie, A.K., Laugesen, P., 2004. The interfacial transition zone (ITZ) between cement paste and aggregate in concrete. Interface Sci. 12, 411–421. https://doi.org/10.1023/B:INTS.0000042339.92990.4c.
Soil Quality Decree [WWW Document], 2015. URL http://wetten.overheid.nl/BWBR0023085/BijlageA/geldigheidsdatum_09-10-2015.
Tang, P., Florea, M.V.A., Spiesz, P., Brouwers, H.J.H., 2015. Characteristics and application potential of municipal solid waste incineration (MSWI) bottom ashes from two waste-to-energy plants. Constr. Build. Mater. 83, 77–94. https://doi.org/10.1016/j.conbuildmat.2015.02.033.
Temuujin, J., Okada, K., MacKenzie, K.J.D., 2002. Zeolite formation by hydrothermal treatment of waste solution from selectively leached kaolinite. Mater. Lett. 52, 91–95. https://doi.org/10.1016/S0167-577X(01)00372-X.
Vollpracht, A., Brameshuber, W., 2016. Binding and leaching of trace elements in Portland cement pastes. Cem. Concr. Res. 79, 76–92. https://doi.org/10.1016/j.cemconres.2015.08.002.
Wei, Y., Shimaoka, T., Saffarzadeh, A., Takahashi, F., 2011. Alteration of municipal solid waste incineration bottom ash focusing on the evolution of iron-rich constituents. Waste Manage. 31, 1992–2000. https://doi.org/10.1016/j.wasman.2011.04.021.
Xi, Y., Siemer, D., Scheetz, B., 1997. Strength development, hydration reaction and pore structure of autoclaved slag cement with added silica fume. Cem. Concr. Res. 27, 75–82. https://doi.org/10.1016/S0008-8846(96)00196-2.
Zhang, Y., Cetin, B., Likos, W.J., Edil, T.B., 2016. Impacts of pH on leaching potential of elements from MSW incineration fly ash. Fuel 184, 815–825. https://doi.org/10.1016/j.fuel.2016.07.089.
Zibara, H., 2001. Binding of External Chloride by Cement Paste. University of Toronto.